Viscous Nongeostrophic Baroclinic Instability

TIMOTHY L. MILLER

Systems Dynamics Laboratory, Marshall Space Flight Center, Huntsville, AL 35812

BASIL N. ANTAR*

Space Science Laboratory, Marshall Space Flight Center, Huntsville, AL 35812

(Manuscript received 8 March 1985, in final form 19 September 1985)

ABSTRACT

Calculations have been performed of the (linear) stability of a baroclinic flow to three-dimensional perturbations. Both the simple Eady basic state and the rotating Hadley cell of Antar and Fowlis are considered. The independent influences of the Richardson (Ri), thermal Rossby (baroclinicity), Ekman, and Prandtl numbers are examined, as well as the influences of the angle of orientation of the horizontal wave vector and the wavelength.

It is shown that if the wavelength is allowed to vary freely, disturbances of the Eady type are preferred (i.e., have greatest growth rate) unless Ri and Ekman numbers are small enough and the thermal Rossby number is large enough. In the latter case, disturbances whose angles of orientation are almost symmetric and whose wavelengths are mesoscale are preferred. If, on the other hand, the wavelength is fixed at a mesoscale size, only the symmetric and almost symmetric modes have growth. By allowing the wave vector orientation to deviate from purely symmetric, we note that the region of instability (i.e., critical Ri) is increased, the extent of which is greater for longer wavelength. For Prandtl number = 1, permitting the angle to be nonsymmetric demonstrates the existence of two maxima in growth rate at opposite angles of orientation and with very different energetics. For Prandtl number far enough from one and for large enough dissipation, only one of these two modes has positive growth rates. Growing oscillatory modes were found for some cases.

1. Introduction

We consider here the stability of a purely baroclinic basic state, with Richardson number (Ri) of order one. Stone (1966) showed that, for Ri small enough (<0.95), the "symmetric" (Solberrg) instability can have larger linear growth rates than the zonal (Eady) instability in the inviscid, hydrostatic situation. (Stone, 1971, and Tokioka, 1970, studied the inviscid nonhydrostatic case, which has only small differences from the hydrostatic one.) The Eady mode (Eady, 1949) is well known to be essentially the source of the extratropical cyclones which have such a profound effect upon weather and upon the general circulation. Although the importance of the symmetric instability is not yet clear, the existence of this phenomenon has been reasonably well established by Emanuel (1983). In that work, a particular case study of mesoscale convective rolls in a baroclinic environment showed that the atmospheric state after the convection had occurred was quite stable to pure buoyant convection (i.e., the vertical lapse rate was less than moist adiabatic) but neutral to the symmetric instability. Other observational analyses (e.g., Bennetts and Sharp, 1982; Parsons and Hobbs, 1983) offer further evidence of symmetric instability in the atmosphere. It has also been suggested that this instability is important in the atmospheres of Jupiter and Saturn (Stone, 1976) and of Venus (Golitsyn, 1984). There remains a need for further theoretical study. In particular, there remain questions about the effects of moisture and about the possibility of enhancing the instability by allowing arbitrary wave vector orientation. The present work addresses the latter topic.

Although the inviscid model of Stone (1966) indicates that only the purely symmetric and purely zonal disturbances need to be considered (for a horizontally infinite channel), the work of Busse and Chen (1981) indicates that, when diffusive effects are considered, the maximum critical Ri for the symmetric mode actually occurs away from the purely symmetric orientation for Prandtl number (Pr) away from one. Busse and Chen could not indicate the extent of the increase in critical Ri, since their conclusions were based upon the first-order results of an expansion in the zonal wavenumber, assumed small. Furthermore, they did not obtain a result for $Pr \equiv 1$. The study by Antar and Fowlis (1983) was of a basic state which included Ekman layers, with an interior approximately in thermal wind balance (for small enough E), and considered fully three-dimensional instabilities. Antar and Fowlis found that, for fixed symmetric wavenumber, the in-

* Permanent affiliation: University of Tennessee Space Institute, Tullahoma, TN.

crease in Ri_c by allowing a nonzero zonal wavenumber is small. Antar and Fowlis also found that the growth rate of the symmetric modes tends to increase as Ri is reduced, and that there *may* be a point where the growth rate of the symmetric (or almost symmetric) mode is greater than that of the zonal mode. However, for Pr = 1 this was not true except for sufficiently small E. Although it would be tempting to explain this by pointing to the lack of "double diffusive" effects for Pr = 1, we note that Antar and Fowlis constrained Ri and the thermal Rossby number (Ro, which measures the baroclinicity) to have a specified relationship by fixing their parameter ΔT, dimensionless vertical temperature difference. In the case of Pr = 1, Ro was reduced as Ri was reduced. The two-dimensional study of Miller (1985) emphasized that the symmetric instability becomes weaker as the thermal Rossby number is decreased in the nonhydrostatic region in parameter space where Antar and Fowlis performed their calculations. We shall see here that this combination of circumstances had considerable effects upon their results, and that herein lies the explanation for the apparently strange behavior at Pr = 1. A study of the simpler—but perhaps more relevant to the atmosphere—hydrostatic case, with fully three-dimensional disturbances, is a major goal of the present work.

The present study elucidates the independent influences of the Richardson, thermal Rossby, Prandtl, and Ekman numbers upon the stability of the basic state, encompassing hydrostatic and nonhydrostatic ranges. Both the pure thermal wind and the Hadley cell models are studied, with most of the detailed calculations made on the former. Three-dimensional disturbances are allowed, with parameters horizontal wavelength and angle of orientation (equivalent to specifying the x and y wavenumbers). Energy conversion integrals are computed for some of the unstable modes. One goal is to suggest where in parameter space one mode may be favored over others according to linear analysis. When the wavelength is constrained to be of mesoscale size, we shall see that *almost* symmetric modes are generally the most favored, and that they are (in a certain sense) two distinct modes. For Pr = 1, both modes may be growing (at approximately the same growth rate, but at different angles of orientation). For Pr sufficiently away from unity, only one mode may be growing. The exactly symmetric modes are actually one of these two modes, depending upon the Prandtl number.

2. Equations and solution methods

a. *Eady basic state*

We consider a rotating flow vertically confined between horizontal plates separated by a distance H, with a constant temperature gradient and geostrophic basic velocity of constant direction and vertical shear. The rotation is about a vertical axis, at rate Ω. We take a coordinate system such that y' (with unit vector $\mathbf{j}$) increases in the direction of the horizontal projection of the density gradient (i.e., "northward"), z' (with unit vector $\mathbf{k}$) is upward, and x' (with unit vector $\mathbf{i}$) is "eastward." For the Eady basic state the temperature field is

$$\bar{T} = T_0 + \beta z' - \gamma y' \tag{1}$$

and the basic state velocity is

$$\bar{U} = U_0 + \frac{g\alpha\gamma}{2\Omega} z' \tag{2}$$

where α is the thermal expansivity, and g is gravity. The value of U_0 is taken to be zero in the present study, and z' is defined to be zero at the middle of the channel. This basic state satisfies the full equations for conducting, no-slip boundaries if we assume that the boundaries move with the basic zonal flow. We allow perturbations to take the form $\exp[-i(kx' - ly')]$. A wave vector is thus defined $-\mathbf{i}k + \mathbf{j}l$. We define the angle that this wave vector makes with the y'-axis to be ϕ. To make discussion of the results easier, and to indicate how the two-dimensional model of Miller (1985) was adapted for this study, we define a new, rotated coordinate system (Fig. 1) such that the new y-axis coincides with the wave vector (and the new x-axis is parallel to the axes of the convection rolls). Thus

$$\left.\begin{aligned} \tan\phi &= k/l \\ x &= x'\cos\phi + y'\sin\phi \\ y &= y'\cos\phi - x''\sin\phi \end{aligned}\right\}. \tag{3}$$

Note that the total wavelength is

$$L = 2\pi(k^2 + l^2)^{-1/2} \tag{4}$$

and that ϕ is positive for counterclockwise rotation of the axes. We take as our time, distance, velocity and

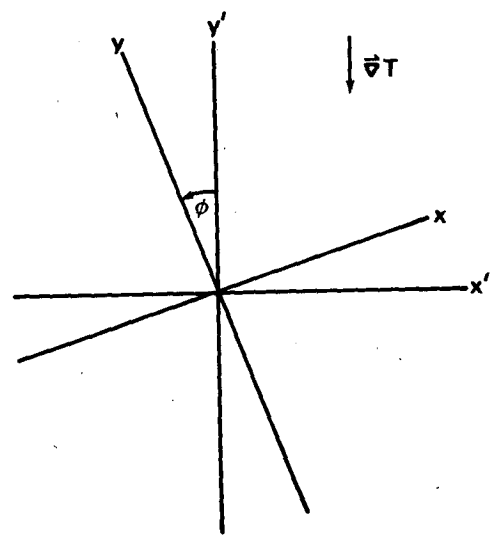

FIG. 1. Coordinate system rotation and orientation with respect to basic state temperature gradient.

temperature scales $(2\Omega)^{-1}$, H, $g\alpha\gamma H/2\Omega$, and γH, respectively. The dimensionless perturbation equations are thus

$$\frac{\partial u}{\partial t} = \mathrm{Ro}\left(z\sin\phi\frac{\partial u}{\partial y} - \cos\phi w\right) + v + E\nabla^2 u, \quad (5)$$

$$\frac{\partial \zeta}{\partial t} = \mathrm{Roz}\sin\phi\frac{\partial \zeta}{\partial y} - \frac{\partial u}{\partial z} - \frac{\partial T}{\partial y} + E\nabla^2\zeta, \quad (6)$$

$$\frac{\partial T}{\partial t} = \mathrm{Ro}\left(z\sin\phi\frac{\partial T}{\partial y} - u\sin\phi - v\cos\phi - \mathrm{RiRo}w\right) + E\,\mathrm{Pr}^{-1}\nabla^2 T, \quad (7)$$

where u, v, and w are the x, y, and z velocity components, T is temperature, and ζ is vorticity $\partial v/\partial z - \partial w/\partial y$. The (no-slip, conducting) boundary conditions are

$$\psi = \frac{\partial \psi}{\partial z} = 0, \quad T = 0, \quad (8)$$

and the dimensionless parameters are

$$\mathrm{Ro} = \frac{g\alpha\gamma}{(2\Omega)^2}, \quad \mathrm{Pr} = \frac{\nu}{\kappa},$$

$$E = \frac{\nu}{2\Omega H^2}, \quad \mathrm{Ri} = \frac{4\Omega^2\beta}{g\alpha\gamma^2}. \quad (9)$$

The streamfunction is defined $\partial\psi/\partial z = v$ and $-\partial\psi/\partial y = \omega$. Note that $\nabla^2\psi = \zeta$; ν is the kinematic viscosity, and κ the thermal diffusivity. The prediction equations are finite differenced in time and in the vertical coordinate (usually 30 increments, with stretching, so that resolution is increased near the boundaries), in the same manner as Miller (1985), and the system is integrated forward in time, with arbitrary initial conditions, until approximately exponential growth occurs. (Initializing with eigenmodes previously computed for a nearby previous point in parameter space often speeds convergence.) Thus a (possibly complex) growth rate is predicted for a given set of parameters Ro, Ri, E, Pr, ϕ, and L. This technique results in convergence only when there is a single fastest-growing (or slowest decaying) eigenmode. When there is a pair of eigenmodes with complex conjugate eigenvalues, the technique fails. In some instances, the shooting method described with the Hadley cell model (section 2b) was used with the Eady basic state to compute eigenvalues when this problem occurred.

Integrated kinetic and potential energy equations are easily derived from the perturbation equations for the velocity components and temperature. (See Miller, 1985.) They are

$$\frac{\partial\langle KE\rangle}{\partial t} = \langle E_1\rangle + \langle E_2\rangle + \langle F\rangle, \quad (10)$$

$$\frac{\partial\langle PE\rangle}{\partial t} = -\langle E_1\rangle + \langle E_3\rangle + \langle D\rangle, \quad (11)$$

where

$$\langle KE\rangle = \left\langle\frac{u^2+v^2+w^2}{2}\right\rangle, \quad (12)$$

$$\langle PE\rangle = \left\langle\frac{T^2}{\mathrm{RiRo}^2}\right\rangle, \quad (13)$$

$$\langle E_1\rangle = \langle wT\rangle, \quad (14)$$

$$\langle E_2\rangle = -\mathrm{Ro}\langle w(u\cos\phi - v\sin\phi)\rangle, \quad (15)$$

$$\langle E_3\rangle = -\frac{1}{\mathrm{RiRo}}\langle T(v\cos\phi + u\sin\phi)\rangle, \quad (16)$$

where $\langle F\rangle$ and $\langle D\rangle$ are the viscous and thermal dissipation terms, and where the brackets $\langle\ \rangle$ refer to volume integration. (Note that RiRo^2 is a static stability parameter S.) The total perturbation energy equation is the sum of Eqs. (10) and (11):

$$\frac{\partial\langle TE\rangle}{\partial t} = \langle E_2\rangle + \langle E_3\rangle + \langle F\rangle + \langle D\rangle. \quad (17)$$

b. Hadley cell basic state

For the Hadley cell calculations, the model and the analysis are those given by Antar and Fowlis (1983). Briefly, the basic state temperature and velocity fields are obtained as solutions to the Navier–Stokes and energy equations, assuming no-slip, corotating horizontal boundaries. Under the parallel flow assumptions, the velocity profiles obtained possess Ekman layers near the horizontal boundaries, with the interior in approximate geostrophic balance, depending upon the Ekman number. Due to the vertical variation of the basic state profiles, the Richardson number is a function of height. At the midpoint it is given approximately by

$$\mathrm{Ri} \approx \frac{\Delta T}{\mathrm{Ro}(1-f')^2} + \frac{\mathrm{Pr}}{(1-f')}, \quad (18)$$

where

$$f' = Re^{-R/2}(\cos R/2 + \sin R/2) \quad (19)$$

and where $R = (2E)^{-1/2}$. Note that for large R, (18) reduces to $\mathrm{Ri} \approx \mathrm{Pr} + \Delta T/\mathrm{Ro}$. The perturbation equations for these basic state profiles are quite complicated due to the variation of the coefficients with height. The linearized perturbation equations with the homogeneous boundary conditions form an eigenvalue problem. This is solved numerically using a shooting method technique with an eighth-order Runge–Kutta–Fehlberg initial value integrator. Convergence on the eigenvalues is obtained through a Newton–Raphson iteration, with orthonormalization of the solution used to overcome the stiffness of the equations. The reader is referred to Antar and Fowlis (1983) for all of the details. Similar to the method of the previous section, a (possibly complex) growth rate is computed for a given set of parameters.

Although we shall show results of calculations with this model for a broad range of Ro, it is noted that modes other than the baroclinic modes may be dominant for large Ro. For example, in his nonlinear calculations Miller (1984) found that the thermal boundary layers can be convectively unstable to small wavelength modes. Furthermore, the laboratory experiments of which the Hadley cell model is an approximation (Miller and Fowlis, 1985) are not easily performed at very large Ro and, simultaneously, at small E. However, we shall show results at large Ro for the purpose of comparison with the Eady basic state model, considering only the (long wavelength) baroclinic modes.

3. Results

a. $Pr = 1$

The upper, solid curve in Fig. 2 is from Miller (1985), and is the critical Ri vs Ro for the symmetric case ($\phi = 0$) for $E = 0.001$ and Pr = 1 for the Eady basic state. As discussed in that paper, the requirement that the critical Ri decrease as Ro decreases is due to the increasing effect of dissipation as the thermal forcing decreases. The region where Ro is large enough that the critical Ri is not a function of Ro is the region where the hydrostatic approximation is valid.

When Ri is decreased from its critical value (fixing the other parameters—except L, which is varied to find the maximum growth rate) the growth rate increases. Except for extremely nonhydrostatic cases, a positive Ri may be found where the growth rate for the symmetric mode just equals that of the zonal mode ($\phi = 90°$), where for both modes the value of L at the maximum growth rate is found. (The wavelength of maximum growth rate for the zonal mode is about eight times that of the symmetric mode.) This Ri exists because the growth rate of the symmetric mode is a much stronger function of Ri than the zonal mode. We shall call this the "transitional" Richardson number, Ri*. The lower solid curve depicts this quantity as a function of Ro. The transitional Richardson number is analogous to Stone's (1966) result for the inviscid, hydrostatic case, for which he found that the symmetric mode is preferred over the zonal mode for Ri < 0.95. Note that the curve for the transitional Ri has a similar shape as the curve for the symmetric critical Ri.

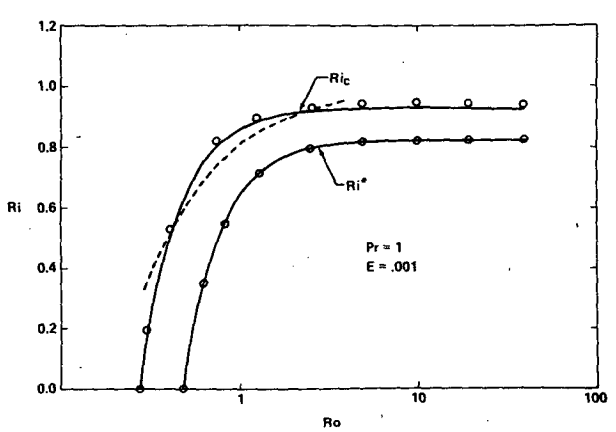

FIG. 2. Critical and transitional Richardson number vs thermal Rossby number for $E = 0.001$, Pr = 1. The solid curves are results for the simple (Eady) basic state, and open circles are for the Hadley cell basic state. The dashed curve is that along which Antar and Fowlis (1983) performed their calculations.

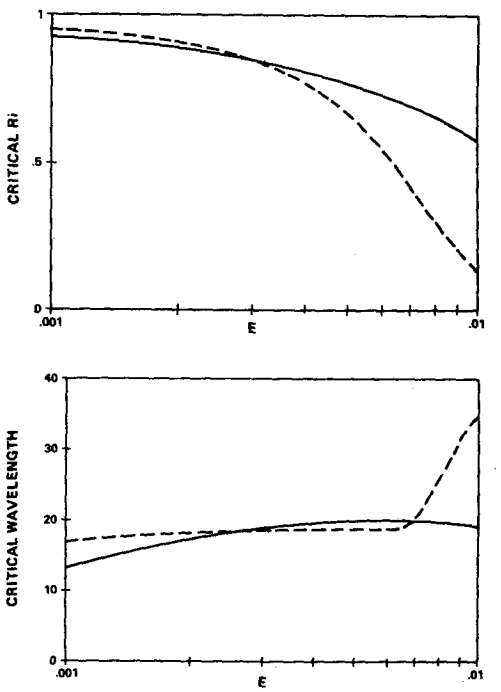

FIG. 3. Comparison of (a) critical Ri and (b) wavelength vs E between the Eady basic state (solid curves) and Hadley cell (dashed curve) models for Ro = 20 and Pr = 1.

The results for the Hadley cell model are also shown in Fig. 2 (open circles). Note that these results almost coincide with those of the Eady basic state. This indicates that, for these values of E and Pr, the Ekman layers in the basic state play no important role in the stability to the modes considered here. As the Ekman number is increased, however, significant deviations between the Ri_c of the two models may be seen at about $E = 0.005$ (Fig. 3). The difference becomes quite large for larger E. Note that the Eady basic state may be regarded as an approximation to the Hadley cell basic state for small enough E, and that as E becomes larger (i.e., as the boundary layers become thicker) this approximation becomes poorer.

Partly because of the added complexity of considering nonhydrostatic cases (because Ri_c and Ri* become functions of Ro), and also because the hydrostatic cases are more relevant to the atmosphere, the remainder of the results shall be for hydrostatic cases, specifically Ro = 20. In Fig. 4 may be seen the results

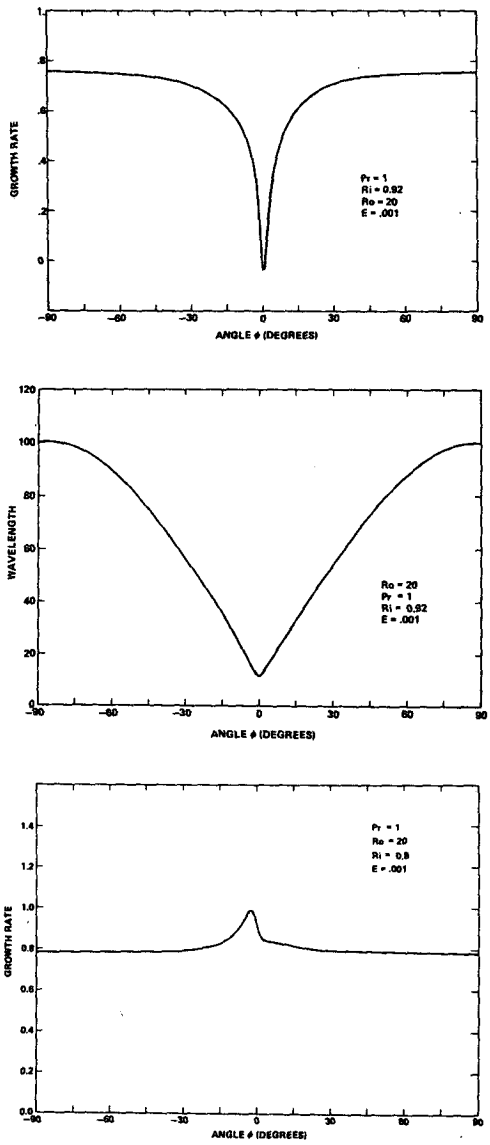

FIG. 4. Results of calculations for Pr = 1, Ro = 20, $E = 0.001$, Eady basic state, with wavelength varied to find that of maximum growth rate. (a) Maximum growth rate vs angle of orientation for Ri = 0.92. (b) Wavelength of maximum growth rate vs angle of orientation for same case as Fig. 4a. (c) As in Fig. 4a, but for Ri = 0.8.

of allowing the angle ϕ to vary throughout the range $-90° < \phi < 90°$ for the Eady basic state. (By "growth rate," we refer to ω, where the form $e^{\omega t}$ is assumed.) Here, the wavelength which gave maximum growth rate was found for each angle (Fig. 4b). For the values of Ri in Figs. 4a, b (slightly unstable for the symmetric mode), there is a very sharp minimum in growth rate (which is actually negative there) at a small, positive ϕ. For Fig. 4c, Ri is less than the transitional Ri*, and there is a growth rate maximum at a small negative ϕ. The wavelength vs ϕ curve corresponding to Fig. 4c is similar to Fig. 4b. Note that the wavelength of maximum growth rate has a sharp minimum at the symmetric point, increasing rapidly away from there.

Figure 5 shows the energy transfer terms as a function of angle of orientation for the case corresponding to Figs. 4a, b. The energetics change rapidly near $\phi = 0$. For $\phi < 0$, inertial transfer ($\langle E_2 \rangle$) dominates, and for all other ϕ buoyant transfer ($\langle E_1 \rangle$ and $\langle E_3 \rangle$) dominate—*except* for $\phi = 0$, where inertial and buoyant transfer are both important. The instabilities for ϕ near 0 are completely different modes for positive and negative ϕ. Furthermore, the energetics of these modes are similar to those for Pr greater than and less than one, respectively, for the symmetric case. (See Miller, 1985, and section 3b.)

We shall now consider results of calculations performed when the wavelength is fixed at some value of "mesoscale" size (i.e., close to the preferred symmetric value), and vary the orientation angle only. Figure 6a shows the growth rate vs ϕ for Ri and L equal to the critical values for the symmetric mode (0.926 and 13.2, respectively). The time-integration technique failed to converge in the region between the two curves shown, because there exists two oscillatory modes with equal decay rate (verified by using the shooting method). Note that there is positive growth for both positive and negative ϕ with maxima at $\phi = 5.0°$ and $-3.5°$, respectively. The growth rate is larger for the negative angle. A "critical" Ri was found for the inertial (negative ϕ) case by increasing Ri to the point where the region of positive growth rate ended (while L was fixed, but ϕ was allowed to vary). The critical Ri was 0.985, and the critical ϕ was $-3.5°$. There is a secondary critical Ri of 0.974 at $\phi = 4.6°$. When L is fixed at 20 (about 50% more than the symmetric critical value), the region of instability is expanded further. In Fig. 6b, Ri is fixed at 1.0. There are maxima in the growth rate at $\phi = -10°$ and $+15°$. The growth rates at these two maxima are approximately the same. When a "critical" Ri is found as before, it is 1.081 at $\phi = +6.5°$; there is a "secondary critical" Ri of 1.050 at $\phi = -6.5°$. (There is actually a third critical Ri and ϕ of 1.047 and $-1°$; the growth rate versus angle curve has two local max-

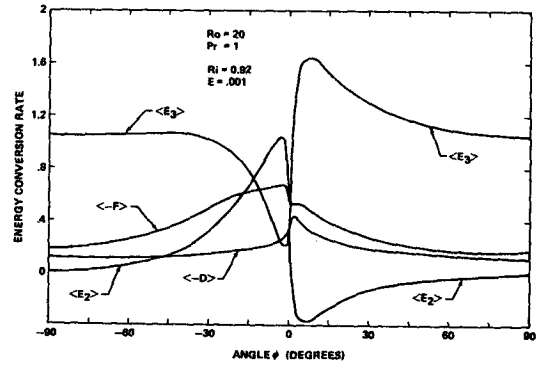

FIG. 5. Energy conversion integrals for the case of Fig. 4a.

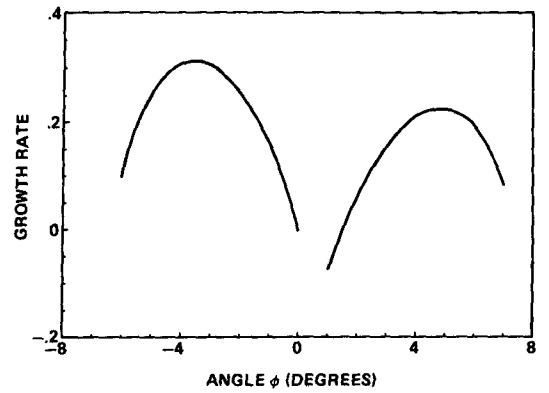

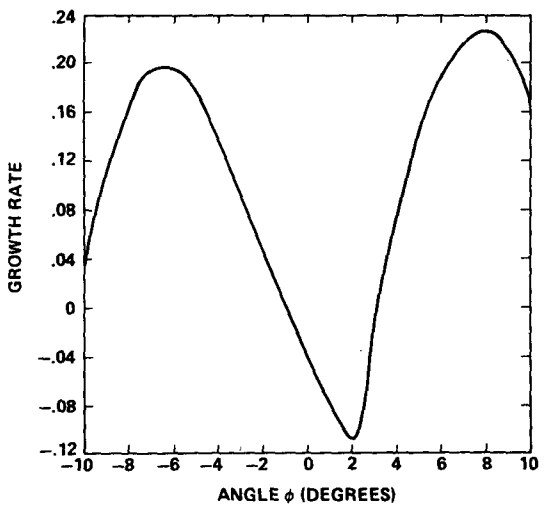

FIG. 6. Growth rate vs angle of orientation for fixed wavelength, for Pr = 1, Ro = 20, E = 0.001, Eady basic state. (a) Growth rate vs angle at the critical Ri (0.926) and wavelength (13.2) for the symmetric case. (b) As in Fig. 6a, but for Ri = 1.0 and L = 20.

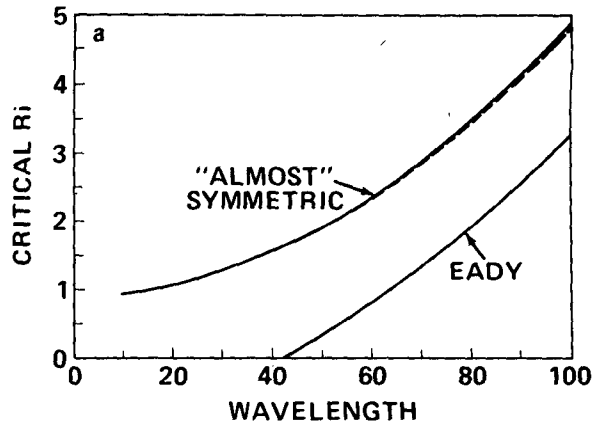

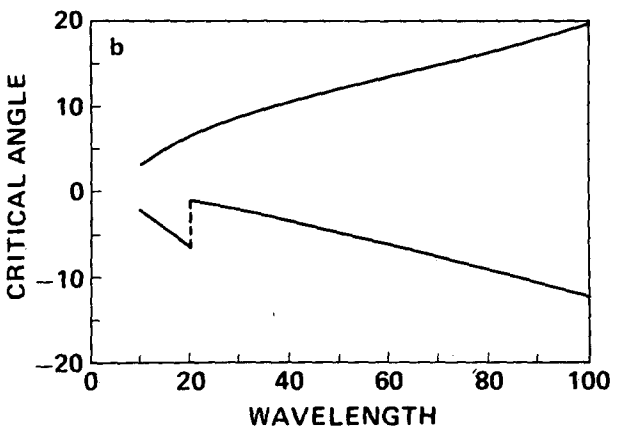

FIG. 7. (a) Critical Ri and (b) ϕ vs wavelength for Pr = 1, E = 0.001, Ro = 20, Eady basic state. In (a) the upper solid curve is for negative ϕ, the dashed curve is for positive ϕ. The lower solid curve in (a) is the critical Ri for the Eady mode (ϕ = 90°).

ima for negative ϕ. The energetics at these two points are similar.) Figure 7 shows the critical Ri and ϕ as functions of wavelength for this set of parameters, up to L = 100. The critical Ri for these "almost symmetric" modes is larger than that for the ϕ = 90° mode, also plotted on Fig. 7a. (Another perspective is that the short-wave cutoff is for smaller wavelength for the almost symmetric mode.) At much larger wavelength than that plotted (L = 1000), there is only one maximum in growth rate, at ϕ = 90° (with critical Ri of 147).

Another set of calculations at the critical point for symmetric instability was performed for smaller E (10^{-4}). Figure 8, in comparison with Fig. 6a, indicates that as the Ekman number becomes smaller, the region of added instability due to the allowance of the 3-D effect shrinks, both in terms of the growth rate and of the angle of orientation. The growth rate maxima are near $\phi = \pm 0.5°$, and the growth rate was negative for $\phi = \pm 1.0°$. This result indicates that the expanded region of instability (by allowing ϕ to be nonzero) shrinks as $E \to 0$, and we recover the results of Stone (1966). Similar calculations for larger dissipation (E = 0.01, not shown) give a single maximum in growth rate for negative ϕ only (at $\phi \approx -12°$ for E = 0.01).

In Fig. 9 may be seen the results of parallel calcu-

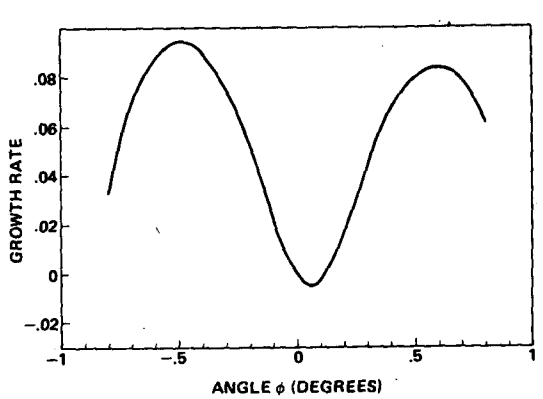

FIG. 8. As in Fig. 6a, but for $E = 10^{-4}$, Ri = 0.984, and L = 5.1.

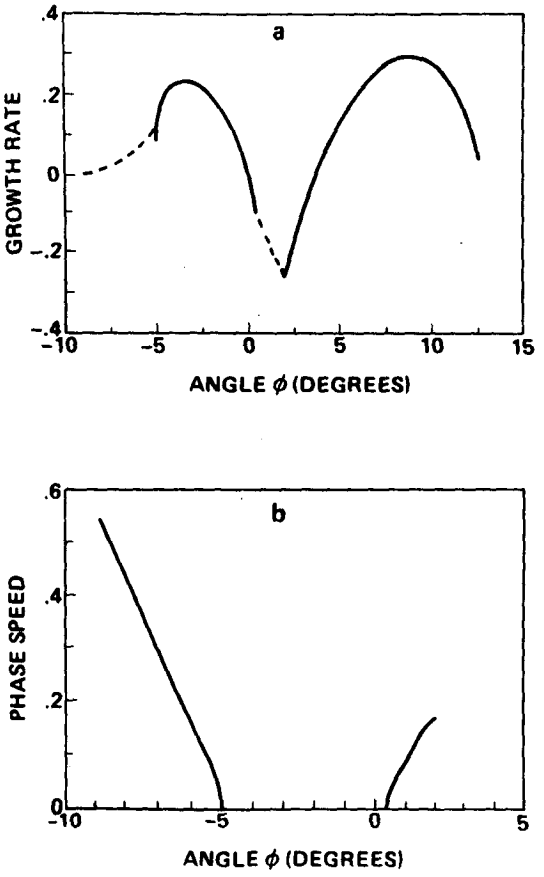

FIG. 9. (a) Growth rate and (b) nonzero phase speed for the Hadley cell basic state, Ro = 20, E = 0.001, Pr = 1, Ri = 0.9446, and L = 16.8. Note that the scales of the ordinates of (a) and (b) are not the same.

lations of the stability of the Hadley cell model. Figure 9a is the growth rate vs angle ϕ for Ro = 20, E = 0.001, and at the critical Ri (0.9446) and wavelength (16.8) for the symmetric case. Note that the growth rate curve for negative ϕ is quantitatively similar to that of the Eady basic state model (Fig. 6a). The growing mode at positive ϕ, however, has a slightly larger maximum growth rate at a significantly larger angle ($\approx$9° vs $\approx$5°) than the corresponding mode of the Eady model. Thus, the Ekman and thermal boundary layers apparently have a significant effect upon the buoyant mode. The results are qualitatively similar, however. Figure 9b shows the imaginary part of the eigenvalue for the oscillatory modes between −9° and −5°, and 0.4° and 2°. (There also exist modes with complex conjugate of that shown.) Note that there is a region of growth of an oscillatory mode for $-9° < \phi < -5°$. This was not found to be the case for the Eady basic state.

b. Pr ≠ 1

The results of calculations for Pr away from one were in some ways similar to the above. The critical Ri for the symmetric case is a function of Ro, with a curve of similar shape to that of Fig. 2 (see Miller, 1985). When Ri is reduced sufficiently (except for extremely nonhydrostatic cases), a transitional Ri may be found, where the growth rates for the symmetric and zonal modes are equal. The wavelength for the zonal instability is much larger than that for the symmetric instability.

When the Richardson number is less than the transitional Ri, and the maximum growth rate is calculated as a function of angle of orientation, the Pr > 1 curves (e.g., Fig. 10, which is for Pr = 2) are qualitatively similar to that for Pr = 1. There is a maximum growth rate at a small positive ϕ, and a growth rate minimum near ϕ = 90°. For Pr < 1, on the other hand (see Fig. 10, which is for Pr = 0.5), the maximum growth rate is for a small negative ϕ, while there is a *minimum* for small positive ϕ. For even smaller values of Pr (e.g., Pr = 0.2), the minimum is very sharp, with a growth rate (it actually can become negative) much below the maximum and below the zonal mode's growth rate. This asymmetry is evidently due to the fact that we are fixing E while varying Pr—i.e., fixing viscosity while varying thermal diffusivity. Decreasing Pr implies increasing thermal diffusivity, and hence the buoyant energy conversion preferred for positive ϕ is suppressed.

The plots of the energy conversion integrals vs ϕ are seen in Fig. 11. The zonal (Eady) mode is buoyant in origin regardless of Pr (the energy conversion integrals for the azimuthal mode are in general very weak functions of Pr), whereas near enough to the symmetric orientation the energy conversion is mostly inertial for Pr = 0.5 and mostly buoyant for Pr = 2. In each of these cases, we see that there do not exist two clearly distinct almost symmetric (fastest-growing) modes as in the Pr = 1 case, although the energetics change very rapidly near ϕ = 0. In the case of Pr = 2 seen in Fig. 11a, inertial energy conversion ($\langle E_2 \rangle$) is approaching

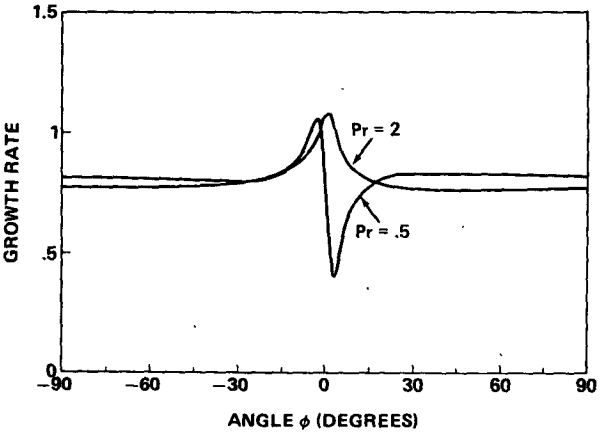

FIG. 10. Maximum growth rate vs angle of orientation for Ri = 0.92, Ro = 20, E = 0.001 and Pr = 0.5 and 2 (Eady basic state).

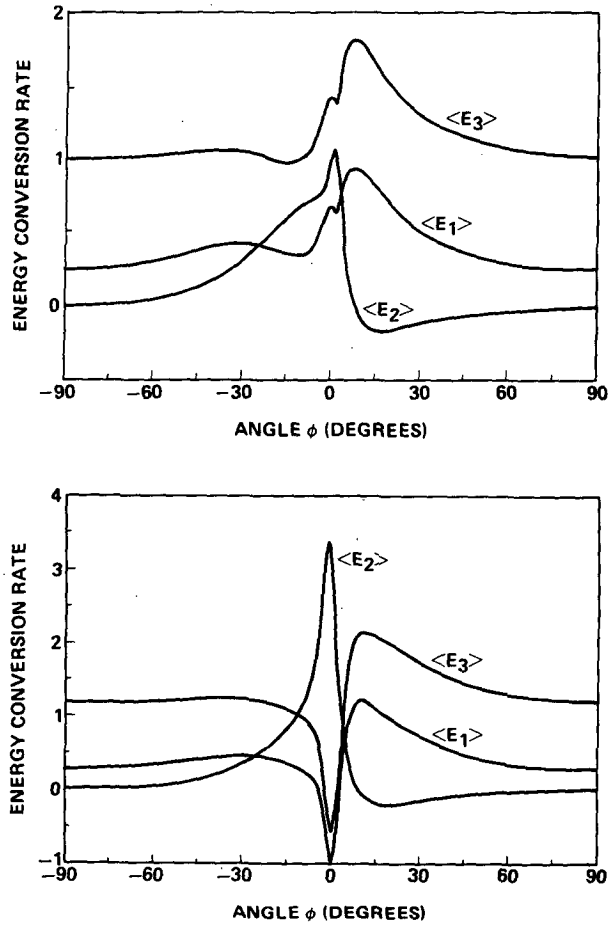

FIG. 11. Energy conversion integrals for the case of Fig. 10. (a) Pr = 2. (b) Pr = 0.5.

$\langle E_1 \rangle$ in importance as a kinetic energy source near the symmetric case. This is not the case for larger Pr (e.g., Pr = 5). Regardless of the value of Pr, the value of $\langle E_2 \rangle$ decreases very rapidly away from $\phi = 0$; there is also a sharp maximum in the magnitude of $\langle F \rangle$ (not shown) near $\phi = 0$ in all cases.

Further differences between cases of different Pr may be seen when the wavelength is fixed and the angle of orientation varied, as in the last part of section 3a. Rather than having maxima in growth rate at both sides of the symmetric angle, there is only one maximum for the nonoscillatory modes, which is at positive ϕ for Pr > 1 and at negative ϕ for Pr < 1. (See Fig. 12.) Again, we see that the inertial mode does not grow for Pr = 2, and the buoyant mode does not grow for Pr = 0.5. It is interesting that growing oscillatory modes were found for Pr = 2, since it raises the possibility that those modes may be fastest growing for some other combination of parameters or in a nonlinear situation. However, these questions are outside the scope of the present investigation. No growing oscillatory modes were found for the Pr = 0.5 case.

4. Discussion and conclusions

We shall briefly summarize the major results of the calculations. Unless stated otherwise, the conclusions are valid for the Eady basic state.

1) When the wavelength is varied freely, either the zonal (Eady) mode or an almost symmetric mode is preferred. The latter is the case when Ri is less than a transitional value, which exists as long as the baroclin-

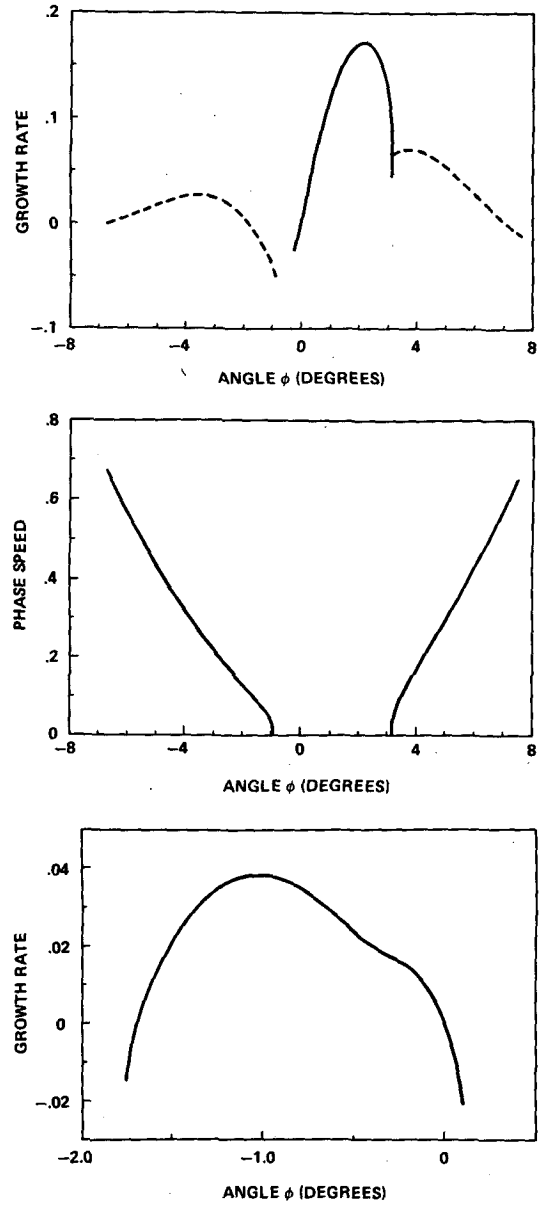

FIG. 12. Growth rate vs angle at the critical Ri(1.03) and wavelengths (16 and 8) for the symmetric cases for Pr = 2 and 0.5, Ro = 20, E = 0.001 (Eady basic state). (a) Growth rate for Pr = 2. The dashed curves are for oscillatory modes, computed using the shooting method. (b) Phase speeds of the oscillatory modes in (a). (c) Growth rate for Pr = 0.5.

icity (Ro) is large enough. The transitional Ri (which, as a matter of great simplification, was computed here by comparing the purely symmetric and zonal modes) is a function of Ro, Pr, and E.

2) When the wavelength and Ri are fixed at or near the critical values for the symmetric problem, exponential growth is possible by allowing the angle of orientation to vary. For Pr = 1, this yields two growing, nonoscillatory modes with approximately equal growth rates, and with angles of orientation of opposite signs. The energetics of these two modes are quite different. For Pr away from one or for large enough E, only one of these modes has positive growth rate.

3) For fixed wavelength, a critical Ri and ϕ may be calculated. Both Ri_c and ϕ_c increase with wavelength. This computation unveils a region of instability of "almost" symmetric modes which can have a critical Ri several times that of the purely symmetric case and which are unstable at a smaller wavelength (or larger Ri at fixed wavelength) than the Eady mode (Fig. 7). For wavelength at the critical value for the symmetric problem, the increase in Ri_c permitted by allowing ϕ to vary is not very large.

4) There exists growing oscillatory modes for some values of the parameters. In the cases computed here, the nonoscillatory modes always had larger growth rate.

5) The Eady and Hadley cell basic states yield similar results in the symmetric instability problem until E is increased to ≈ 0.005. Details in the differences between the two cases at larger E were not investigated.

Some comments on the results of Antar and Fowlis (1983) in light of the present results are appropriate. It was stated in the Introduction that Antar and Fowlis constrained Ri and Ro to have a specified relationship by fixing their ΔT (which depended upon Pr), and that they worked in the nonhydrostatic range. That is, the range in which they worked was (referring to Fig. 2) where Ri_c and Ri* are strong functions of Ro. The combination of these facts had strong effects upon their results. For example, for Pr = 1 and for $E = 0.0005$—their E was defined differently than the present one—they found that the growth rate of the symmetric mode actually decreased as they decreased Ri, and that there never was a point where the growth rate of the symmetric mode overtook that of the zonal mode. This also would have occurred for $E = 0.001$. By inspecting the curves in Fig. 2, we see that as they decreased Ri, they proceeded along a curve in (Ri–Ro) space that never intersects the Ri* curve and, in fact, intersects the Ri_c curve twice, indicating that the growth will at some point decrease with decreasing Ri. When they sufficiently decreased E, however, they found that the growth rate increased with decreasing Ri and a transitional Ri was found. This is because the Ri_c and Ri* curves in Fig. 2 move to the left and upward as E is decreased (i.e., the region where the symmetric mode has larger growth rate is expanded). Thus, the curve along which they worked eventually fell inside an Ri* curve. That this behavior (of decreasing growth rate with decreasing Ri) was observed for Pr = 1 and not for other values of Pr was, in a certain sense, fortuitous, a result of the particular ΔT's (i.e., the particular Ri vs Ro relationships) they chose. Note also that if they had fixed Ro, rather than ΔT, they would have worked along vertical lines in Fig. 2, and their results would have been very different (and would have depended upon the particular Ro chosen, since they worked in the nonhydrostatic region).

The question arises of the physical explanation for the preference of angles of orientation away from symmetric. The inviscid result of Stone (1966) is that the most unstable orientation is exactly symmetric, and the most unstable wavelength is (the limit) zero. When dissipation is included in the equations, modes with finite wavelength are most unstable. Here, we find that these modes prefer an angle of orientation away from symmetric. Of course, with finite dissipation and wavelength there is no reason why an exactly symmetric orientation should be preferred. Busse and Chen (1981) had discovered the preference for nonsymmetric orientations for $\mathrm{Pr} \neq 1$, and for small dissipation. Most of their explanation offered is applicable to a situation with differential diffusion of angular momentum and heat. They concluded that the preferred angle of orientation is such that trajectories lie closer to the plane wholly containing the basic state density and angular momentum gradients (the "meridional" plane). This would increase the efficiency of both the inertial and buoyant energy conversion mechanisms. When the present authors consider the flow direction at the middle of the channel for some of our fastest growing eigenmodes, we agree that the flow direction has a smaller angle to the meridional plane than does the exactly symmetric mode. That is, the v' magnitude is increased more than the u' magnitude. This appears to be true regardless of Pr (including Pr = 1). In all cases, the increase in growth rate is due to an increase in the size of the major energy source term in (17), rather than to a decrease in an energy sink term.

In a situation where there is no external constraint upon wavelength, both synoptic scale and mesoscale modes are unstable for small enough Ri. This will result in a competitive situation, where both modes may be competing for the same energy source. Since the growth rates for the mesoscale modes are strongly dependent upon Ri, and since in a contained, viscous situation, the mean Ri will tend to be increased by the instabilities [shown by Miller (1984) for the symmetric instabilities, and inferred from Williams (1971) for the Eady-type instabilities], it may be expected that the synoptic scale instabilities (of the Eady type) will be observed in a fully nonlinear situation. This was the tentative conclusion of the laboratory experiments of Miller and Fowlis (1985). In those experiments, the symmetric (or almost symmetric) instability was never observed, re-

gardless of the smallness of Ri or the value of the other parameters. Instead, the synoptic-scale baroclinic instability was present. As Ri was reduced to the point of being negative, the flow became an apparent mix of baroclinic instability and convection of the Rayleigh–Bénard type.

The applicability of the present results to the dynamics of the earth's atmosphere is not clear, since effects such as latent heat release are only crudely included. (We have effectively assumed that the entire region is saturated.) Furthermore, the results are obtained by using the Laplacian (viscous) operator in the equations, with constant diffusion coefficients. As far as the atmosphere is concerned, this contains the assumption of isotropic turbulence within the flow. The Prandtl number = 1 results are most applicable within the context of this assumption. In the atmosphere, radiation and the movement of water particles (resulting in regions of unsaturated air, even when the entire region is initially saturated) might cause heat to be a less nearly conserved quantity than momentum. One may speculate, then, that the $Pr < 1$ results may be applicable. Attempting to directly apply these results to the atmosphere is, in any case, dangerous. However, the present results certainly raise the question of whether the often-made symmetric assumption is valid. For example, an alternative explanation to that of Emanuel (1985) of the observations of the continuation of rainbands even after the atmosphere had been rendered neutral to the exactly symmetric instability (Sanders and Bosart, 1985) is suggested. The present results further suggest that there is a possibility in the atmosphere for baroclinic instabilities with a spectrum of scales ranging from mesoscale to synoptic scale, with wave vector orientations ranging from "symmetric" to "azimuthal." The orientation of the instabilities would be determined by the size of the unstable region, except when the potential vorticity is negative enough that "almost" symmetric instabilities are most unstable.

Some other important questions that remain about the instabilities studied here are concerned with nonlinear effects: How do the mesoscale modes evolve in a fully nonlinear three-dimensional situation, where the buoyant and inertial modes compete with each other? What are the effects of this evolution upon the basic state? The nonlinear study of Miller (1984) considered only one orientation (purely symmetric), and thus showed the nonlinear effects of the modes separately. His results were probably highly influenced by the fixed temperature condition on the horizontal boundaries, which effectively imposed an average wind shear with the result that the ultimate energy conversion in all cases was buoyant in origin. A more refined study would examine the three-dimensional effects as well as the effects of the boundary conditions.

Finally, it should be noted that the assumption of constant horizontal temperature gradient is inconsistent with the set of calculations made with a fixed (mesoscale) wavelength. It would be interesting to attempt to verify the qualitative validity of the present results against a basic state where there is a region of small Richardson number of mesoscale size embedded within a synoptic scale flow of large Ri. Another interesting set of calculations would be to consider a basic state where the horizontal temperature gradient (and wind shear) changes direction with height. Both of these studies would possibly shed more light on the extent that the mesoscale instabilities studied here might be expected to be active in the atmosphere.

Acknowledgments. The authors are grateful to Professor Kerry Emanuel for comments on the original manuscript, and to the NASA Office of Space Science and Applications, Global Scale Atmospheric Processes Research Program, for support and encouragement of this research.

REFERENCES

Antar, B. N., and W. W. Fowlis, 1983: Three-dimensional baroclinic instability of a Hadley cell. *J. Fluid Mech.*, **137**, 425–447.

Bennetts, D. A., and B. J. Hoskins, 1979: Conditional symmetric instability as a possible explanation for rainbands. *Quart. J. Roy Meteor. Soc.*, **105**, 945–962.

——, and J. C. Sharp, 1982: The relevance of conditional symmetric instability to the prediction of mesoscale frontal rainbands. *Quart. J. Roy. Meteor. Soc.*, **108**, 595–602.

Busse, F. H., and W. L. Chen, 1981: On the (nearly) symmetric instability. *J. Atmos. Sci.*, **38**, 877–880.

Eady, E. T., 1949: Long waves and cyclone waves. *Tellus*, **1**, 33–52.

Emanuel, K. A., 1979: Inertial instability and mesoscale convective systems. I. Linear theory of inertial instability in rotating viscous fluids. *J. Atmos. Sci.*, **36**, 2425–2449.

——, 1983: On assessing local conditional symmetric instability from atmospheric soundings. *Mon. Wea. Rev.*, **111**, 2016–2033.

——, 1985: Frontal circulations in the presence of small moist symmetric stability. *J. Atmos. Sci.*, **42**, 1062–1071.

Golitsyn, G. S., 1984: Some problems of Venus' atmospheric dynamics. *Icarus*, **60**, 289–306.

McIntyre, M. E., 1970: Diffusive destabilization of the baroclinic circular vortex. *Geophys. Fluid Dyn.*, **1**, 19–57.

Miller, T. L., 1984: The structures and energetics of fully nonlinear symmetric baroclinic waves. *J. Fluid Mech.*, **142**, 343–362.

——, 1985: On the energetics and nonhydrostatic aspects of symmetric baroclinic instability. *J. Atmos. Sci.*, **42**, 203–211.

——, and W. W. Fowlis, 1985: Laboratory experiments in baroclinic instability with heating and cooling on the horizontal boundaries. *Geophys. Astrophys. Fluid Dyn.* (in press).

Parsons, D. B., and P. V. Hobbs, 1983: The mesoscale and microscale structure and organization of clouds and precipitation in midlatitude cyclones. XI: Comparisons between observational and theoretical aspects of rainbands. *J. Atmos. Sci.*, **40**, 2377–2397.

Sanders, F., and L. F. Bosart, 1985: Mesoscale structure in the megalopolitan snowstorm of 11–12 February 1983. Part I: Frontogenetical forcing and symmetric instability. *J. Atmos. Sci.*, **42**, 1050–1061.

Stone, P. H., 1966: On non-geostrophic baroclinic instability. *J. Atmos. Sci.*, **23**, 390–400.

——, 1971: Baroclinic instability under non-hydrostatic conditions. *J. Fluid Dyn.*, **45**, 659–671.

——, 1976: The meteorology of the Jovian atmosphere. *Jupiter*, T. Gehrels, Ed., University of Arizona Press, 586–618.

Tokioka, T., 1970: Non-geostrophic and non-hydrostatic stability of a baroclinic fluid. *J. Meteor. Soc. Japan*, **48**, 503–520.

Williams, G. P., 1971: Baroclinic annulus waves. *J. Fluid Mech.*, **49**, 417–449.